Available online at www.sciencedirect.com
SCIENCE DIRECT®
Journal of Nuclear Materials 346 (2005) 185–193
journal of nuclear materials
www.elsevier.com/locate/jnucmat

Immobilization of cesium in alkaline activated fly ash matrix

A. Fernandez-Jimenez [a,*], D.E. Macphee [b], E.E. Lachowski [b], A. Palomo [a]

[a] *Inst. Eduardo Torroja (CSIC), c/Serrano Galvache s/n, 28033 Madrid, Spain*
[b] *Department of Chemistry, University of Aberdeen, Old Aberdeen AB24 3UE, Scotland, UK*

Received 7 December 2004; accepted 27 June 2005

Abstract

The immobilization potential of alkaline activated fly ash (AAFA) matrices for cesium has been investigated. The presence of Cs in the AAFA pastes, prepared using 8M NaOH solution as activator, showed no significant adverse effects on mechanical strength or microstructure, nor were significant quantities of Cs leached following application of the Toxic Characteristic Leaching Procedure (TCLP) and American Nuclear Society (ANS) 16.1 leaching protocols. Microstructural analysis shows Cs associated with the main reaction product in the AAFA suggesting that cesium is chemically bound rather than physically encapsulated. It is proposed that cesium is incorporated into the alkaline aluminosilicate gel, a precursor for zeolite formation.

1. Introduction

Portland cement-based systems have long been identified as candidate matrices for the solidification and isolation of low- and intermediate level radioactive wastes. These are relatively low-cost, readily available, easy-to use binders, compatible with aqueous waste streams and are capable of activating several chemical and physical immobilization mechanisms for a wide range of inorganic waste species. Despite their widespread use in this role, Portland cement-based materials are not very effective in the treatment of alkali metal wastes and cesium immobilization in particular has proved difficult [1–4]. Cesium −137 is a significant component of radioactive waste from the nuclear industry and its high solubility in water makes it extremely mobile.

The reported success of hydrothermal studies, in which Cs from highly alkaline (pH > 13) solution is incorporated in crystalline aluminosilicate minerals [5–8], prompted the present study which seeks to investigate the efficacy of alkali-activated fly ash cements as alternative binders for waste immobilization. A number of factors are relevant. Alkaline activated fly ash cements have some similarities with Portland cement and other ceramic materials [9,10]. For example, alkaline activated fly ashes set at low temperature (45–150 °C) to give amorphous to semicrystalline structures [11,12] from which zeolite crystallisation may occur in the final stages of hydration. The first-formed aluminosilicate gel product is essentially amorphous to X-rays but NMR [11] studies have revealed a three-dimensional short-range structure in which the Si is found in a variety of environments, with a predominance of $Q^4(3Al)$ and $Q^4(2Al)$ units. Also, alkaline activated aluminosilicates materials are reported to be more durable in aggressive environments [13] than Portland cements. Consequently it is thought that most of industrial and even nuclear wastes

* Corresponding author. Tel.: +34 1 3020440; fax: +34 1 3020700.
E-mail address: anafj@ietcc.csic.es (A. Fernandez-Jimenez).

0022-3115/$ - see front matter © 2005 Elsevier B.V. All rights reserved.
doi:10.1016/j.jnucmat.2005.06.006

(liquids, sludges, solids, etc.) could be stabilized in this type of matrix [6,14–17].

With these considerations, the objectives of the present study were: (i) to determine the effect of cesium salts (CsOH and $CsNO_3$) on the mechanical properties and mineralogical composition (including identification of any zeolitic host phases) of the alkali activated fly ash matrix, and (ii) to determine the effect of curing time (5 h and 7 d) and temperature (85 ° and 120 °C) on leaching behaviour.

2. Experimental

A complete chemical, physical, mineralogical and microstructural characterization of the Spanish class F fly ash used has been reported elsewhere [18,19]; chemical analyses data only are reproduced here in Table 1. The fly ash used is a vitreous material with some minor crystalline phases (mullite, quartz, magnetite and hematite) and is made up of cenospheres and plerospheres with 78.5 wt% of particles sized less than 45 μm.

All samples were activated with 8 M NaOH solution, with a fly ash/solution ratio = 0.4. The cesium content of mixes was kept constant at 1 wt% of the initial fly ash content, and was added as $CsOH \cdot H_2O$ (strongly alkaline base which can attack glass) and $CsNO_3$ dissolved in the alkaline activator. Pastes were mixed by hand to give complete homogenization. They were then poured and compacted into metal moulds. Samples were then sealed in polypropylene bottles and cured in an oven for 5 h and 7 d at temperatures of 85 °C or 120 °C. After curing, the samples were removed from the oven and demolded. Table 2 summarises the compositions of the matrices, and the curing conditions studied.

Prismatic test samples ($10 \times 10 \times 60$ mm) were prepared in order to determine flexural strength (ENE 80-101-91) and the pore size distribution was studied by mercury intrusion porosimetry (Micromeritics 9320). The microstructural characterization of pastes was by means of X-ray diffraction (XRD), Fourier Transform Infrared spectroscopy (FTIR), and scanning and transmission electron microscopy (SEM and TEM). The experimental conditions and procedures for these studies have been reported previously [18–20].

The performance of the different matrices for cesium immobilization was evaluated using two standard leaching methods:

Total characteristic leaching procedure (TCLP): [14,15,21]. Prismatic specimens ($10 \times 10 \times 60$ mm) were ground and sieved to provide particle sizes in the range 4.5–9.5 mm. The leach test was carried out with 100 g of sample and 2 l of fluid #2 [21], prepared by diluting 5.7 ml of glacial acetic acid in 1000 ml of deionised water to give a pH of 2.88 ± 0.05. Solid and leachant are put into a tightly closed vessel with constant agitation for 18 h at 22 ± 3 °C. Liquid and solid phases were then

Table 1
Chemical composition of fly ash

	PF	IR	SiO_2	Al_2O_3	Fe_2O_3	CaO	MgO	SO_3	K_2O	Na_2O
Fly ash	1.80	0.40	51.51	27.47	7.23	4.39	1.86	0.15	3.46	0.70

IR = Insoluble Residue.

Table 2
Matrices compositions and the curing conditions

Sample	Fly ash (g)	1% Cs	8M NaOH (g)	Curing T[a] (°C)	Time
FA.85 °C.5 h	100	0	40	85	5 h
FA.85 °C.7 h	100	0	40	85	7 d
FA.120 °C.5 h	100	0	40	120	5 h
FA.120 °C.7 d	100	0	40	120	7 d
FA1H.85 °C.5 h	100	1.26 g $CsOH \cdot H_2O$	40	85	5 h
FA2H.85 °C.7 d	100	1.26 g $CsOH \cdot H_2O$	40	85	7 d
FA3H.120 °C.5 h	100	1.26 g $CsOH \cdot H_2O$	40	120	5 h
FA4H.120 °C.7 d	100	1.26 g $CsOH \cdot H_2O$	40	120	7 d
FA5N.85 °C.5 h	100	1.47 g $CsNO_3$	40	85	5 h
FA6N.85 °C.7 d	100	1.47 g $CsNO_3$	40	85	7 d
FA7N.120 °C.5 h	100	1.47 g $CsNO_3$	40	120	5 h
FA8N.120 °C.7 d	100	1.47 g $CsNO_3$	40	120	7 d

1% of Cs = 10000 ppm of Cs.

separated. The relative concentrations of Cs, Si, Al, Na, and Fe were determined by ICPMS (ICP-MS, Spectromass 2000).

American Nuclear Society method ANS 16.1: [7–15]. A series of cylindrical samples was prepared (16 mm long × 6 mm diameter), cured (as described above) and placed in a tank with deionised water (leachate). The leachate was removed and replaced at 0.0084 (30 s), 2, 7, 24, 48, 72, 96, 120, 336, 504, 1176, 2160 h. The Cs content was analysed by ion chromatography (CX 500 Dionex with conductivity detector CD40).

3. Results and discussion

3.1. Mechanical strength

Flexural strength data are reported in Table 3 for the different matrices (11 prisms per composition were tested). In general the mechanical strengths increase with the curing time increase, but no significant differences are observed with respect to the curing temperature. However we can observe in both cases (FAH and FAN samples) that the presence of Cs reduces the mechanical strength. This effect is more significant when Cs is adding as $CsNO_3$, probably due to lower pH with respect to Cs as $CsOH \cdot H_2O$ it is well known that pH level is a determining factor in the alkali activation process of aluminosilicates materials [16,22].

To determine the effect of time and temperature of curing in AAFA pastes, the total porosity and the pore size distribution of samples without Cs were determined (see Fig. 1). These results show that, in general, matrices cured at 85 °C and 120 °C have similar total porosities after 5 h curing (the numbers are not sufficiently different to claim a temperature effect) but after 7 d, the 85 °C specimens have lower overall porosity. Also the curing time, as expected, has an influence in the pore size distribution. Matrices cured for 5 h have a higher percentage of pores size between 10 and 0.1 μm, while fly ash matrices cured for 7 d have a higher percentage of small pores between 0.1 and 0.01 μm.

Table 3
Flexural strength

Time	Flexural strength (MPa) of AAFA samples					
	FA.85 °C	FA.120 °C	FAH.85 °C	FAH.120 °C	FAN.85 °C	FAN.120 °C
5 h	2.76 ± 0.4	3.70 ± 0.5	2.6 ± 0.36	3.22 ± 0.38	1.84 ± 0.24	2.35 ± 0.21
7 d	11 ± 0.73	9.43 ± 0.96	7.38 ± 0.74	8.38 ± 0.94	5.07 ± 0.67	8.67 ± 0.62

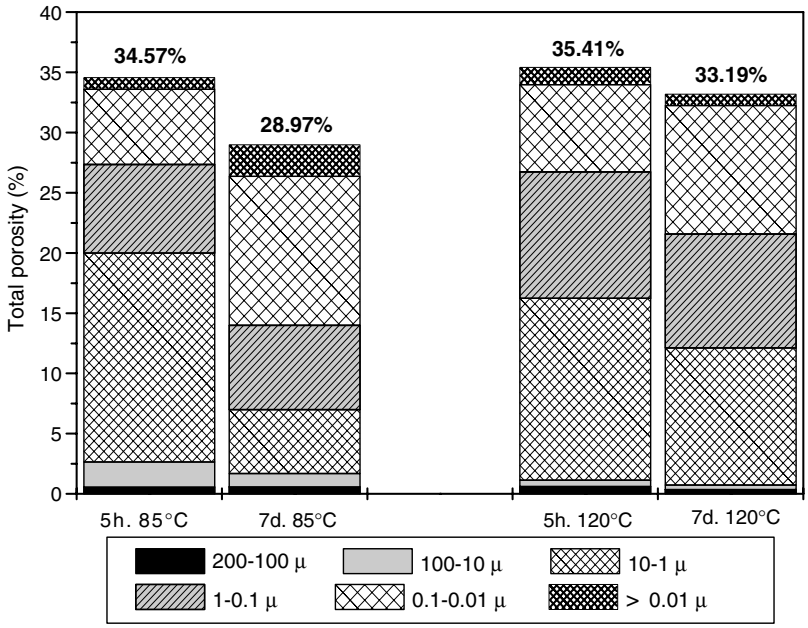

Fig. 1. Total porosity and pore size distribution.

3.2. Mineralogical and microstructural characterisation

XRD patterns of alkaline activated fly ash pastes, with and without cesium, are presented in Fig. 2 as a function of the reaction time and temperature. According to the XRD data the original fly ash consists mainly of a glassy phase (see the broad hump between 20° and 30° 2θ) with some minor crystalline phases (mullite, quartz and magnetite) (see Fig. 2 and Table 4).

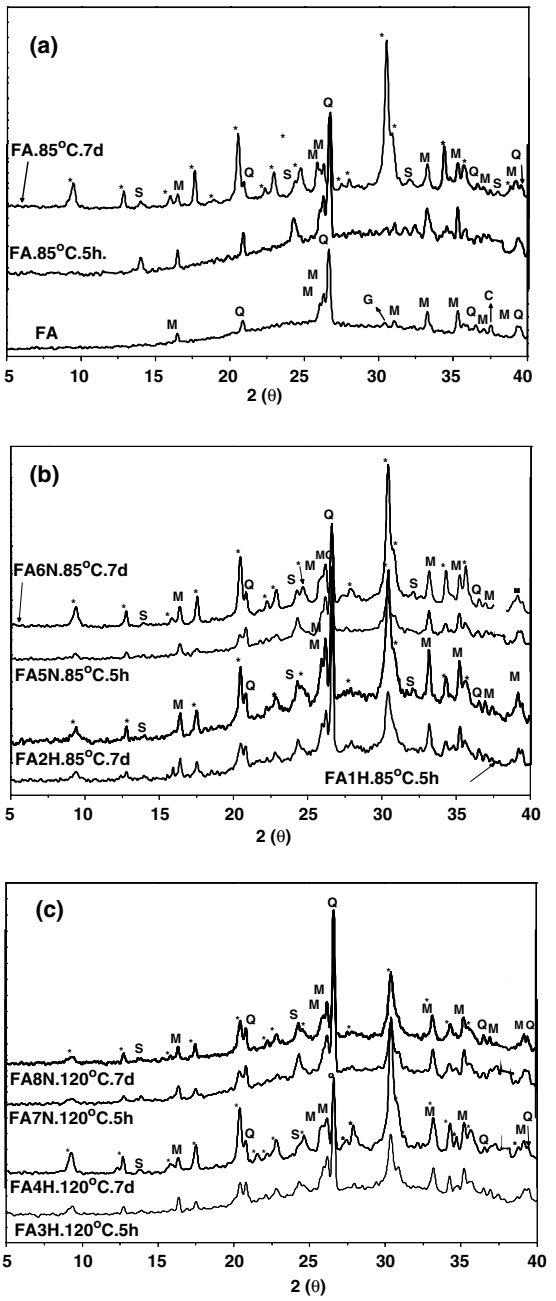

Fig. 2. XRD spectrum of (a) un-reacted FA and AAFA pastes without Cs, curing at 85 °C; (b) AAFA pastes with Cs curing at 85 °C and (c) AAFA pastes with Cs curing at 120 °C (for captions see Table 4). Q = Quartz; M = Mullite; G = Hematite; C = CaO; S = hydroxysodalite; * = herchelite.

Evidence of fly ash reactivity is apparent after only 5 h at 85 °C (Fig. 2(a)). The amorphous contribution to the XRD pattern has increased, indicated by a broadening of the amorphous 'hump', suggesting that the initial product (alkaline aluminosilicate gel) is also poorly crystalline. Also some new minor crystalline phases are detected with peaks at positions consistent with hydroxysodalite and herschelite (See Table 4 where the relevant XRD data are presented). With continued reaction, the intensity of these peaks increases and the amorphous character of the diffraction pattern diminishes. The 5 h data indicate crystallisation of hydroxysodalite but herschelite peaks were not confirmed until later; they were identified after 20 h curing (data for 20 h are not shown but the relevant peaks are evident in the 7 d data).

In the presence of Cs, a similar picture emerges in relation to the evolution of new peaks consistent with hydroxysodalite and herschelite formation. However, in these cases, the patterns do not tend to reduce in amorphous character with increased curing time (Fig. 2(a) and (b)).

It is reasonable to propose that the incorporation of cesium in the system could involve some substitutions Cs–Na in the products of reaction giving rise to some differences in peak position and intensity of those products in the XRD spectra. This could be explained by the greater scattering potential of cesium and to the larger ionic radius of cesium which would affect crystallographic cell parameters and redefine peak positions. However, reference to literature data [3,5] indicates that cesium-like zeolites such as Cs-herschelite, Cs-hydroxysodalite, pollucite etc., have XRD patterns with peaks in positions very similar to those developing peaks observed for the AAFA pastes; it is difficult to distinguish all of the peaks due to peak overlap in the AAFA patterns. A further difficulty arises due to the relatively small Cs loading and the patterns only permit characterization of that fraction of the total hydrated system which has crystallised. It is confirmed by the amorphous humps in all of the patterns for Cs-containing systems that most of the hydrates have not crystallised so that Cs associated with the amorphous gel did not contribute to the crystalline zeolites discussed above. It is therefore not possible, through XRD alone, to derive a quantitative assessment of the degree of Cs substitution (for Na) in the crystalline (zeolite) hydrates from the AAFA system.

The corresponding FTIR data are shown in Fig. 3. The spectra for fly ash show the three wide bands characteristic of aluminosilicates. The band appearing at

Table 4
XRD references and annotate patterns

Elements	Symbol	JCPDF	2(θ) value/intensity			
Quartz SiO_2	Q	5-490	26.64 (100)	20.83 (34)		50.17 (17)
Mullite $Al_6Si_2O_{13}$	M	15-776	26.26 (100)	25.96 (94)		40.86 (60)
Hydroxysodalite $Na_4Al_3Si_3O_{12}OH$	S	11-401	24.50 (100)	14.09 (80)		35.01 (80)
Herschelite $NaAlSi_2O_6 \cdot 3H_2O$	[a]	19-1178	30.50 (100)	20.55 (65)	45 (50)	24.73 (20)
Pollucite[a]		29-0407	26.05 (100)	24.3 (50)		30.68 (45)
$CsAlSi_2O_6 \cdot xH_2O$[a]		25-194	26.05 (100)	30.69 (45)		24.38 (30)

[a] The main reflection of these phases can be masked by some of the reflections belonging to other minerals present in the system.

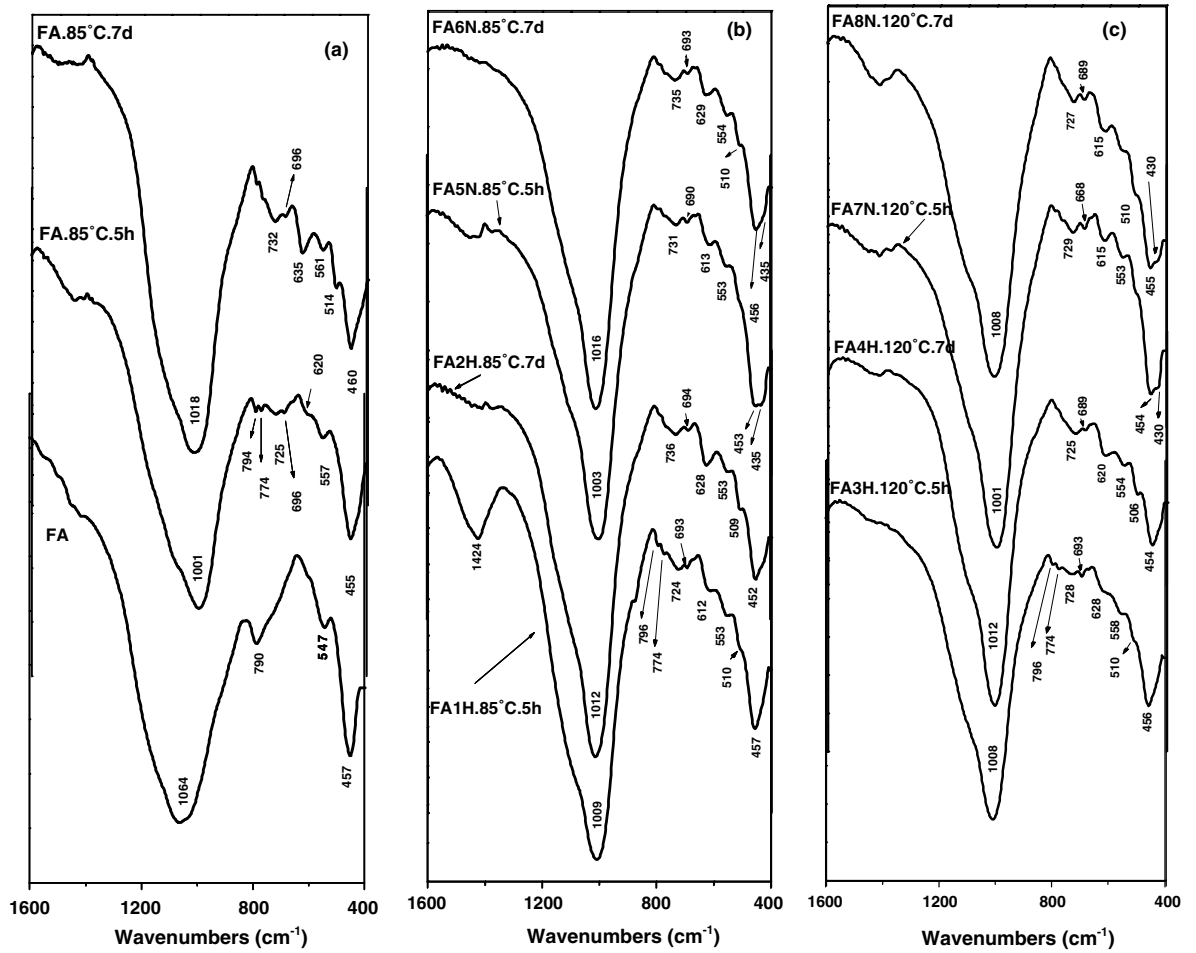

Fig. 3. FTIR spectrum of (a) un-reacted FA and AAFA pastes without Cs, curing at 85 °C; (b) AAFA pastes with Cs curing at 85 °C and (c) AAFA pastes with Cs curing at 120 °C.

1064 is associated with T–O (T = Al, Si) asymmetric stretching vibrations. The band at 457 cm^{-1} is associated with T–O bending vibrations. The band appearing at 780–790 cm^{-1} corresponds to the quartz present in the original fly ash and the band at 547 cm^{-1} corresponds to mullite.

In the spectra of AAFA pastes (Fig. 3(a)) the band associated with T–O stretching vibrations shifts to lower

frequencies (to 1000–1010 cm^{-1} at 5 h and to 1010–1020 cm^{-1} at 7 d). The shift in absorption frequency is related to compositional effects (Al/Si ratio [20,23]); the initial effect is associated with an Al-rich intermediate reaction product, which gradually enriches in Si to slightly shift the band towards higher frequencies. The presence of Cs appears not to influence this behaviour significantly (Fig. 3(a) and (b)).

The FTIR data are however consistent with the occurrence of zeolites as indicated by XRD, although they do not permit distinction between the amorphous aluminosilicate product and the crystalline aluminosilicate zeolites, which may be considered to be the final stage of evolution of the system in all matrices of Fig. 2. The bands appearing between 800 and 500 cm^{-1} can be identified with the tetrahedral secondary building units (SBU) and fragments of the aluminosilicate system [24,25]. The band appearing at around 720–730 cm^{-1} may be associated with Al-rich structures such as hydroxysodalite [20].

According to the literature, the band at 640–630 cm^{-1} observed for zeolite structures can shift towards lower frequencies due to distortions in the ringed connections (single 6-membererd ring (S6R) or double, 6-membered ring (D6R)) between SBU's [23–25]. The ultimate explanation for this lies in the different M–O bond energies associated with differences in Al^{3+} and Si^{4+} ionic radii. The influence of counter ions (Cs^{+} or Na^{+}) adds to this distortion potential so that the band appearing at 640–630 cm^{-1} may provide clues to possible substitutions in the zeolite structure. Zeolites of the chabazite family (e.g. herschelite-type zeolite as detected in the AAFA hydration products) have D6R connections and have corresponding FTIR absorbances at around 520–510 cm^{-1} and 640–630 cm^{-1}. The observed shift of these absorbances to slightly lower frequencies in Cs-loaded samples may suggest possible Cs^{+} substitution for Na^{+} in these structures.

Fig. 4 shows SEM images of alkali activated fly ash mortars hydrated with solutions of $CsOH \cdot H_2O$ and $CsNO_3$ respectively and cured for 7 d at 85 °C. The heterogeneous morphology is made up of intact or broken hollow spheres (cenospheres) corresponding to partially reacted fly ash, and hydration products. Fig. 4(a) shows a relatively large, partially reacted fly ash grain (centre) in a matrix of hydration product. Other smaller grains are also evident but the large, hollow grain contains smaller crystallites, having rosette-like textures, within. Fig. 4(b) shows these products in more detail. Within the fly ash rim, evident around the periphery of the image, several crystallites have formed and are agglomerated. Based on EDX analysis and morphology, it is suggested that these crystalline rosettes are aluminosilicate zeolites and that the mass from which they are emerging is an amorphous precursor form having similar composition. However, the main reaction product is the aluminosilicate gel whose composition is expressed in average atomic ratios: for FA2H.85 °C.7 d (points 1, 2), Si/Al = 1.9–2.0 and Na/Al = 0.9–1.0; for FA6N.85 °C.7 d (points 4, 5) Si/Al = 2.0–2.1 and Na/Al = 0.9–1.

Analysis of the crystalline materials, e.g. point 3 gives Si/Al = 1.95 and Na/Al = 0.96. Point 6 to Si/Al = 2.16 and Na/Al = 0.81 are consistent with compositions expected for the zeolite herschelite. Note also that Cs was detected in these crystalline structures but only when cesium was introduced to the system as $CsOH \cdot H_2O$.

Fig. 5 shows transmission electron micrographs of the alkaline activated fly ashes matrices. The familiar spherical morphologies of the fly ash particles are again evident as discs, amongst other features including hydration rims and the protuberances associated with them. With this technique more detail can be derived both from morphological and compositional information, the latter being available from energy dispersive X-ray

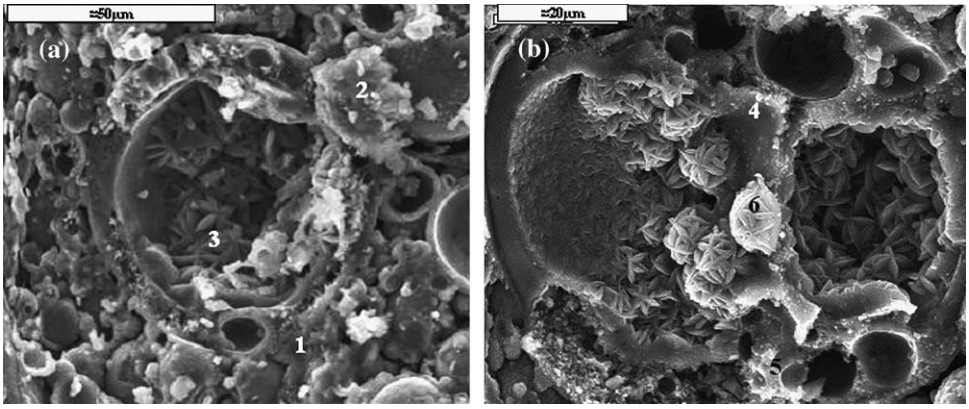

Fig. 4. (a) Sample FA2H.85 °C.7 d (with $CsOH \cdot H_2O$) (points 1–3) and (b) sample FA6N.85 °C.7 d (with $CsNO_3$) (points 4–6).

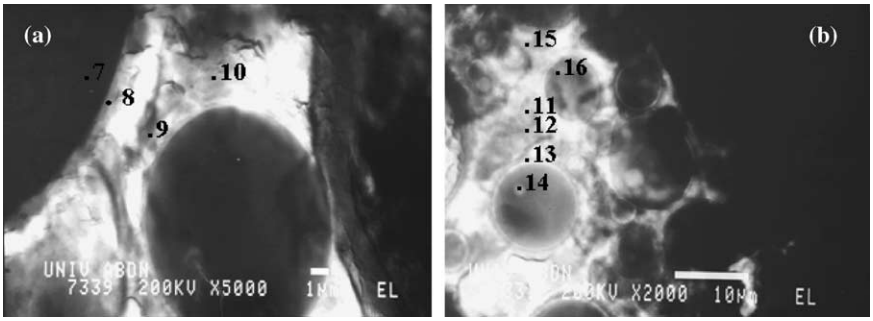

Fig. 5. (a) Sample FA3H.120 °C.5 h and (b) sample FA5N.85 °C.5 h.

analysis (EDX). Transmission microscopy is capable of providing the resolution necessary to focus on small microstructural features enabling microanalysis within hydration rims. Such information is useful in correlating compositions with specific morphologies.

Fig. 6 summarises the raw analytical data obtained from EDX acquired from the points numbered 7–16 in Fig. 5. The values are expressed as atomic percentages normalised from all the elements analysed (Na, Al, Si, S, K, Ca, Ti, Fe and Cs) and take no account of the presence of oxygen or water. Although they are not absolute percentages they are, nevertheless, a useful indicator of relative amounts. Note that the penetration of beam electrons into the specimen at these points may lead to interaction of the electrons with underlying phases although analytical points were chosen to minimise such interferences. Also the electron diffraction showed that the main reaction product was amorphous.

Fig. 6 suggests that the composition associated with the point 15 is predominantly an alkaline aluminosilicate

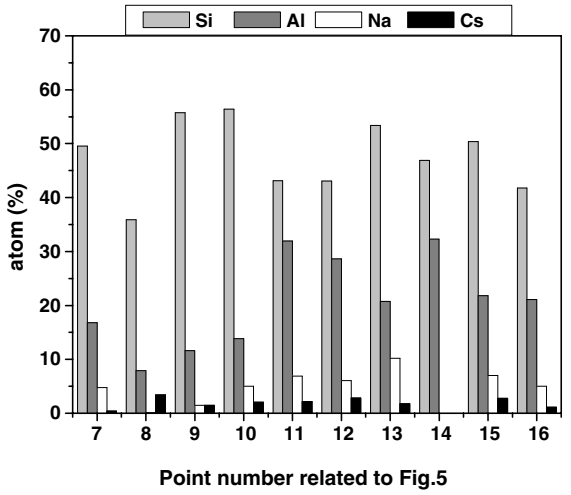

Fig. 6. EDX data AAFA paste. For clarity, only Al, Si, Na and Cs data are shown.

with Si/Al = 2.3, Na/Al = 0.32 and Na + Cs/Al = 0.45. Note the lower level of Na and Cs detected can be due to the high volatility of these elements in this type of analysis.

With this technique, it evident when considering the immobilization potential of this type of matrix that cesium appears to be associated basically with the reaction product. The highest relative cesium concentration in any of the analyses (see Fig. 6) is associated with points 8–13, 15 and 16. All of these correspond to positions within (or close to) the matrix and in the reactions rims of fly ash particles.

3.3. Leaching programme

Leachate Cs concentrations following the ANS 16.1 leaching test were consistently below the analytical detection limit (1 ppm). However, the dynamic TCLP method show that only low levels of Cs were leached from all of AAFA matrices studied (Table 5). As previously reported [12,14,15,19,26], these matrices are robust to aggressive leachants and the low levels of Al and Si in leachates confirm this again. Although the concentrations of Cs introduced to the AAFA matrices were small, the low leachate concentration suggests that these matrices may be suitable for Cs immobilization. In

Table 5
Leaching results obtained by TCLP method

Samples	Leaching elements			
	Si (%)	Al (%)	Na (%)	Cs (%)
FA1H.85 °C.5 h	0.34	0.11	16.75	0.45
FA21H.85 °C.7 d	0.35	0.20	12.70	0.25
FA3H.120 °C.5 h	0.73	0.30	28.27	1.30
FA4H.120 °C.7 d	0.40	0.32	24.05	0.69
FA5N.85 °C.5 h	0.76	0.60	27.56	1.21
FA6N.85 °C.7 d	0.38	0.30	16.25	0.22
FA7N.120 °C.5 h	0.77	0.30	30.53	1.44
FA8N.120 °C.7 d	0.37	0.28	15.90	0.42

general, with increased reaction time, the available Cs for leaching appears to be reduced as indicated by the decrease in the percentage of Cs leached. This is most likely to be due to an increase in the degree of reaction with consequent increase in hydration products with binding capacity for Cs, but may also be a consequence of microstructural effects, e.g. reduction of pores between 10 and 0.1 μm and increases the percentage of small pores (between 0.1 and 0.01 μm, see Fig. 1).

Comparing these data with those in the literature [2,3] the retention of Cs appears to be more effective in alkali-activated fly ash and other aluminosilicates matrices than for OPC-based systems. According to Hoyle and Gruzeck [3] the amount of cesium leached from the waste forms decreased as the alumina and/or silica content of the formulations increase. This may be due to a reduction in the degree of connected porosity which is characteristic of such systems or to an increase in the chemical/physicochemical binding of Cs in/on hydration products. The better retention of Na in/on low C/S C–S–H than on high C/S ratio C–S–H is well known as well as the good cation retention in condensed aluminosilicate structure. The main reaction product in AAFA is an alumino silicate gel with a 3D structure [11]. From compositional considerations alone, the silica/alumina rich – surface charges in the gel are more negative in the system investigated here than in lime-rich gel (C–S–H from OPC) and so are potentially better as adsorbing cations.

Differences in the availability of Cs to leach out of the matrix are evident only at early age. Samples aged 5 h and cured at 85 °C containing Cs as $CsOH \cdot H_2O$ have higher strengths, appear to develop higher level of zeolite formation and lower levels of Cs leached (and also of Si, Al and Na) than samples activated with $CsNO_3$. The reason for this behaviour may be related to the relative alkalinity of the salts. When the CsOH is added to the 8M NaOH solution, the pH of the solution is not significantly affected. The addition of $CsNO_3$ has an acidifying effect (due to NO_3^-) and may have an inhibiting effect on the hydrolysis kinetics (hydration rate) in these mixes. This study has already highlighted some important differences between the basic and acidic additions (see Table 3 for example, where lower mechanical strength are obtained with $CsNO_3$). This effect is small because the concentration in all cases is low. Consequently the effects are more evident at the earlier age. The effect is less significant in the more mature samples.

In all case the cesium content leachated decreases with the curing time, indicating that cesium may be being partitioned into the reaction products of AAFA. Alternatively, these observations would be consistent with Cs entrapment in fluid-filled isolated porosity, because both the total porosity and the pore size decrease with the curing time (see Fig. 1). The increased leaching of Cs (and other mobile ions) at higher temperatures may be attributable to the coarser pore structure arising from the higher temperature curing.

The hydrated system comprises a poorly crystalline aluminosilicate gel, with some minority crystalline phases of zeolite type. These coexist with a liquid phase residing in the pore space. During hydration, ions in the mixing water are partitioned between the hydrating solid phases and the remaining pore solution, the partitioning being driven by equilibrium considerations. When the matrix becomes subject to leaching, leachant penetrates through connected porosity to interact with solids and mass transport is then controlled by dissolution/precipitation/sorption and diffusion processes. Ions weakly associated with solids are leached first and contribute to high initial leachate concentrations. Conversely, low leach rates imply either strong binding to solids or encapsulation in disconnected or isolated porosity. In the present study, the identification of zeolites having retention capacity for Cs encourages the view that some immobilization potential (rather than physical encapsulation) is active in this system, although the anticipated ion-exchange mechanism opens a route to Cs release (if an ion more suitable to the exchange site becomes available in penetrating leachant).

To better understand the immobilization mechanisms for Cs in these matrices, studies involving higher concentration of cesium are needed. This would increase confidence in interpretation of the analytical data, which in the present study was restricted by detection limits (ANS leach test, XRD interpretation).

4. Conclusion

The main conclusions of this work are:

- Neither mechanical strength nor microstructure of AAFA matrices were significantly affected by incorporation of Cs.
- Only small amounts of Cs are leached from this type of matrix. Results obtained suggest that the cesium is chemically incorporated into the reaction product. There is an apparent association of cesium with the alkaline aluminosilicate gel or 'zeolite precursor', the main reaction product in the AAFA.
- At early ages, a higher level of Cs is leached from matrices in which Cs is introduced as $CsNO_3$ than as CsOH. This may be because CsOH is a more active base and increases the initial reaction rate to secure a more consolidated microstructure and a higher volume of reaction product.
- Finally due to the absence of distinct hydrated Cs compounds (e.g. CsOH, $CsNO_3$) within the reaction products, we believe that the percentage of cesium fixed is therefore chemically bound rather than physically encapsulated.

Acknowledgements

To the Royal Society/CSIC for awarding a grant associated with this research, also to the Regional Government of Madrid for awarding a post-doctoral grant. The Spanish Directorate General of Scientific Research for funding the project COO-1999-AX-038 associated with this research. Also, thanks to M. Alonso and A. Raab for your help in the chemical analysis.

References

[1] D.E. Macphee, F.P. Glasser, Mat. Res. Soc. Bull. 18 (1993) 66.
[2] C.E. McCulloch, A.A. Rahman, M.J. Angus, F.P. Glasser, R.W. Crawford, in: Advances in Ceramics, in: G.G. Wicks, W.A. Ross (Eds.), Nuclear Waste Management, vol. 8, American Ceramic Society, Columbus, OH, 1984, p. 113.
[3] S.L. Hoyle, M. Grutzeck, J. Am. Ceram. 72 (10) (1989) 1938.
[4] A.M. El-Kamash, A.M. El-Dakrounry, H.F. Aly, Cem. Concr. Res. 32 (2002) 1797.
[5] M.J. Lambregts, S.M. Frank, Micropor. Mesopor. Mater. 64 (2003) 1.
[6] M.Y. Khalil, E. Merz, J. Nucl. Mater. 211 (1994) 141.
[7] M. Calligaris, A. Mezzetti, G. Nardin, L. Randaccio, Zeolites 6 (1986) 137.
[8] P. Bosch, D. Caputo, B. Liguori, C. Colella, J. Nucl. Mater. 324 (2004) 183.
[9] F.P. Glasser, Br. Ceram. Trans. J. 89 (1990) 195.
[10] A. Palomo, A. Fernández-Jiménez, M.T. Blanco-Varela, Polímeros Minerales Alcalinos, VIII Congreso Nacional de Materiales, Valencia, Spain, 2004, pp. 25–30 ISBN: 84-9705-594-2.
[11] A. Palomo, S. Alonso, A. Fernández-Jiménez, I. Sobrados, J. Sanz, J. Am. Ceram. Soc. 87 (6) (2004) 1141.
[12] A. Palomo, A. Fernández-Jiménez, M. Criado, Mater. Construcc. 54 (275) (2004) 77.
[13] A. Palomo, M.T. Blanco-Valera, M.L. Granizo, F. Puertas, T. Vazquez, M.W. Grutzeck, Cem. Concr. Res. 29 (1999) 997.
[14] A. Palomo, M. Palacios, Cem. Concr. Res. 33 (2003) 289.
[15] A. Fernandez-Jimenez, D.E. Macphee, E.E. Lachowski, A. Palomo, J. Am. Ceram. Soc. 88 (5) (2005) 1122.
[16] J.W. Phair, J.S.J. Van Deventer, Miner. Eng. 14 (3) (2001) 289.
[17] J.G.S. Van Jaarsveld, J.S.J. Van deventer, A. Schwartzman, Miner. Eng. 12 (1) (1999) 75.
[18] A. Fernández-Jiménez, A. Palomo, Fuel 82 (2003) 2259.
[19] A. Fernández-Jiménez, A. Palomo, E.E. Lachowski, D.E. Macphee, Cem. Concr. Compos. 26 (2004) 1001.
[20] A. Fernández-Jiménez, A. Palomo, Micropor. Mesopor. Mater., in press.
[21] J.R. Conner, Chemical Fixation and Solidification of Hazardous Wastes, Van Nostrand Reinhold, New York, 1990.
[22] S. Alonso, A. Palomo, Mater. Lett. 47 (2001) 55.
[23] M. Sitarz, W. Mozgawa, M. Handke, J. Mol. Struct. 511&512 (1999) 281.
[24] M. Sitarz, M. Handke, W. Mozgawa, Spectrochim. Acta Part A 56 (2000) 1819.
[25] W. Mozgawa, M. Sitarz, M. Rokita, J. Mol. Struct. 511&512 (1999) 251.
[26] A. Fernández-Jiménez, A. Palomo, M. Criado, Cem. Concr. Res. 35 (2005) 1204.